

ORIGINAL RESEARCH PAPER

Structural and Morphological Characterization of Nanocellulose Extracted from Cotton Straw Residue

Sheetal, Savita Sihag, Monika Yadav, Jitender Pal*

Department of Environmental Science and Engineering, Guru Jambheshwar University of Science and Technology, Hisar-Haryana, India

Received: 2021-11-12

Accepted: 2021-12-22

Published: 2022-02-01

ABSTRACT

This study is focused on the synthesis and characterization of cotton straw residue. Nanocellulose was synthesized by chemical method and followed by ultrasonication and cryocrushing. The results of the present study show that the cotton straw residue consists of lignin (27%), hemicellulose (15%), cellulose (32%), and ash content (2.3%). Nanocellulose was characterized by FTIR, XRD, FESEM, TEM, DSC, TGA, and AFM. Two aromatic rings were observed at wavelength 1650.47cm^{-1} and 1436.53cm^{-1} which indicates that there is a presence of cellulose in the prepared sample which was characterized by FTIR. The structural analysis shows that the material was amorphous and the nanocellulose crystallinity is 23%. The morphological analysis using FESEM indicates even elongated fiber with a smooth surface and it contains pore in the nanocellulose of cotton residue. TEM analysis indicates that nanocellulose has an irregular shape with a circular rod-like structure of different sizes. The enthalpy of nanocellulose changes at 168.48°C due to endothermic transition. TGA results show that the nanocellulose is degraded in the temperature range $300\text{-}355^\circ\text{C}$ and low thermal stability was observed during the experiment. AFM result shows the needle shape particle (root square mean roughness = 0.1738nm) and the size of nanocellulose was observed 7.1 nm .

Keywords: Nanocellulose, Cotton Fiber, Acid Hydrolysis, Cryocrushing, Nanocellulose characterization, Agriculture waste.

How to cite this article

Sheetal, Sihag S., Yadav M., Pal J., Structural and Morphological Characterization of Nanocellulose Extracted from Cotton Straw Residue. J. Water Environ. Nanotechnol., 2022; 7(1): 1-13.

DOI: [10.22090/jwent.2022.01.001](https://doi.org/10.22090/jwent.2022.01.001)

INTRODUCTION

Cotton is one of the most important commercial cash crops in India which is produced in more than 12 states and Gujarat is the leading cotton-producing state in India. Major cotton-producing nations are China, USA, Pakistan, India, Uzbekistan, Australia, Egypt, Argentina, Greece, etc. India holds 1st rank in the refinement of cotton fiber [1]. Cotton crop residue has many other applications such as fuel for cooking food and fodder for animals [2], pulp and paper [3], energy production [4], heavy metal removal [5], removal of organic matter [6], etc. A few researchers have used effectively cotton crop

residue in order to upgrade soil nourishment to further develop crop usefulness by utilizing rice-based harvest practices [7].

Cotton straw consists of constituents such as lignin, cellulose, and hemicellulose. Cellulose is a straight-chain polysaccharides unit made up of numerous glucose monosaccharide units which are linked with $\beta(1-4)$ linkage of the D-glucose unit with a hydrogen bond [8]. Cellulose could be extracted from a diversity of sources such as firewood, bast filaments, greenswards, bud fiber, seed strings, invertebrates, microorganisms, etc. These sources are mainly categorized into industrial and agricultural waste [9]. Hemicellulose has

* Corresponding Author Email: j_pal2k1@yahoo.com

distinct monosaccharide units of glucose, galactose, mannose, xylose, and arabinose which are isomers of each other [10]. Lignin which is a complex structure derived from wood and an integral part of the secondary cell wall of the plant acts as gluing the cellulose units together. It helps in water transportation, provides mechanical strength, and is insoluble in water [11-12]. Hemicellulose is allied with hydrogen bonds and lignin with a covalent bond [13]. Lignin, cellulose, and hemicellulose are interlinked which shows that the fiber is arranged in a crystalline and disorderly manner as shown in Fig. 1.

Various extraction methods of nanocellulose such as mechanical (High-pressure homogenization [14], chemical methods, hammer milling [15], Cryocrushing, high shear homogenization [16-17], high-speed blending [18], micro-fluidization [19], grinding [20] high-intensity ultrasonication [21], and alive enzymes [22] are reported in the literature.

In Northern states, mainly Haryana, after harvesting cotton crops, a lot of residues which include stalks, locules, cotton bolls, leaves, and roots are left in the fields. In the absence of adequate sustainable management practices, a huge quantity of residue is being burnt on-farm to clear the field for sowing the next rabi crops (mainly wheat and mustard). Crop residue burning has become a major environmental challenge that causes health issues due to the emission of CO₂, CO, CH₄, NO_x, and SO_x which is contributing to global warming [23].

This research paper mainly emphasizes the utilization of cotton crop straw for nanocellulose extraction by the chemical method followed by ultrasonication and Cryocrushing. It also focuses on how we overcome the cotton crop residue burning problem to minimize global warming and

the best utilization of cotton crop residue.

Novelty of research

In the absence of an adequate sustainable management plan for the reuse of agro-waste, the farmers burn their crop residue on the farm in huge quantities. This burning of the crop has many environmental problems caused by the emission of various gases which results in global warming and climate change. Due to the facts mentioned above, the present study was conducted in order to handle crop residue by extracting cellulose from the agricultural biomass.

MATERIALS AND METHODS

Materials

The cotton straw (Bt-cotton) was collected, cut into small pieces, and washed with tap water. The raw material was washed and dried in sunlight. After drying, the same was grinded and sieved from a 80µm size sieve. The raw powder sample was oven-dried and kept in PVC bottles for further treatment. AR grade chemicals were used in the whole experimentation.

Estimation of Lignocellulosic constituents

Cellulose, hemicellulose, lignin, and ash content were evaluated according to Goering and Van Soest method (1991) [24-25].

Synthesis of Nanocellulose

The powder raw sample was soaked into 4% (w/v) sodium hydroxide (NaOH) and stirred at 80°C for 2 hr. pH level was increased by adding NaOH, and to maintain their pH, the sample was washed with double distilled water. At last, strained excess of cotton straw was collected and alkaline treatment refine hemicellulose and lignin.

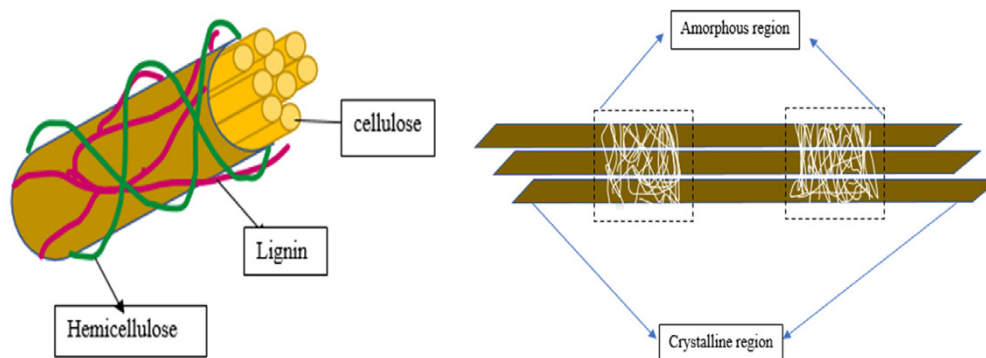


Fig. 1. The binding pattern and structure of lignocellulosic biomass

In bleaching treatment, the filtrate of the previous experiment was treated at 80°C by subsequently adding sodium hypochlorite (NaOCl) 80% (w/v) solution until the bleached white fiber was attained and this process was repeated 4 to 5 times. The sample was cooled, filtered, and washed with distilled water till the pH of the sample become neutral. A white color bleached cellulose fiber was collected and dried at 40-50°C in a hot oven for 10-12 hours. This action liberates lignin and other impurities from the processed sample. To extract nanocellulose fiber, acid hydrolysis was given to cellulose fiber to disrupt the severe arrangement of cellulosic constituents. A 40%(w/v) H₂SO₄ was added to the bleached cellulose fiber and was heated at 40°C for 1 hour. To obtain nanocellulose fiber, the sample was washed with distilled water 4 to 5 times to remove excess acid and maintain the pH neutral. In the sonication process, water was separated from the sample of nanocellulose fiber at 60°C for 1 hour and then further centrifuged the sample at 4000 rpm. After centrifugation, the Cryocrushing process was accomplished to increase the further surface area of nanocellulose fiber in the nanometer. The Liquid Nitrogen (LN₂) was added which solidify the sample and then immediately crushed the material with mortar and pestle. The sample was dried and stored in a PVC bottle for further characterization. Fig. 2 showed the extraction process of nanocellulose.

Characterization of cotton straw nanocellulose Fourier Transform Infrared Spectroscopy(FTIR)

FTIR is an analytical technique that is used by a material analyst to know a substance's chemical composition. Perkin Elmer spectrums, BX-II (FTIR) spectrophotometer were used. Spectra were recorded of raw material, alkali-treated, bleached and acid hydrolyzed material.

The different processed samples were mixed with KBr, mechanically grinded, and formed a film. Spectrum was obtained in the range of 4400-500 cm⁻¹.

Structural property(XRD)

X-ray diffraction (XRD) was performed on a Rigaku Miniflex-II diffractometer at room temperature with a copper anti cathode operated at 40 kV and 40 mA to check whether the structure of samples is crystalline or amorphous. Diffraction was executed on power samples spread smoothly on a neutral quartz glass sample holder and expose

k-alpha radiation source and scanned in the range of 10° to 80° at 2 theta angles. The Segal method was used to calculate the crystallinity index (CrI) [26][26].

$$CrI = \frac{I_{(002)} - I_{(AM)}}{I_{(002)}} \times 100$$

Where: (002) is the extreme crystallinity value and (am) is for the amorphous part of the sample. Higher intensity is diffracted at an angle 2θ = 22° and low-intensity peak is scattered at 2θ = 18° angle.

Microscopic study

Field Emission Scanning electron microscope (7610F plus/JEOL) was used to analyze the shape, dimension surface morphology of the sample. The sample was assessed at two stages before and after the chemical treatment. The voltage was accelerated at 30 kV and the sample was coated with sputter coater before treatment. TALOS HR-TEM (ThermoFisher) at 200 kV was used to analyze TEM for particle size and shape and their morphology.

Differential Scanning Calorimeter (DSC)

Three mg of sample were placed in the platinum container and heated from 0 to 400°C at 5°C/min in a helium atmosphere. Thermo-analysis was performed on Q-10, TA Instruments Waters.

Thermal Gravimetric Analysis (TGA)

To know the thermal degradation, the sample was analyzed by using SDT Q 600 thermogravimetric equipment. The temperature range for analysis was 25°C-900°C at a heating rate of 10°C/min under a nitrogen atmosphere (10ml/min).

Atomic Force Microscopy (AFM)

The sample was treated with methanol/ethanol mix for dissolving. Bruker multimode 8 AFM was used for AFM analysis.

RESULT AND DISCUSSIONS

Mechanism of lignocellulosic biomass

The raw cotton straw has 27% lignin, 32% cellulose, 15% hemicellulose, and 2.3 % ash content (shown in Table 1). For nanocellulose extraction, the raw material was chemically treated. The alkaline treatment(Sodium hydroxide) removes a certain amount of lignin and hemicellulose



Fig. 2. Extraction of nanocellulose

Table 1. Lignocellulosic biomass content in Percent (%)

| Crop Residue | Lignin | Cellulose | Hemicellulose | Ash content | References |
|--------------|--------|-----------|---------------|-------------|---------------|
| Cotton stalk | 29.4 | 40.10 | 13.60 | - | [27] |
| Corn straw | 07.3 | 42.04 | 41.02 | - | [29] |
| Cotton stalk | 30.9 | - | - | 1.8 | [15] |
| Rice straw | 19.64 | 38.6 | 19.7 | 18.67 | [30],[31] |
| Wheat straw | 18.8 | 52.4 | 18.2 | 3.7 | [32] |
| Bagasse | 20-30 | 32-48 | 19-24 | 1.5-5 | [33] |
| Cotton straw | 27.0 | 32.0 | 15.0 | 2.3 | Present study |

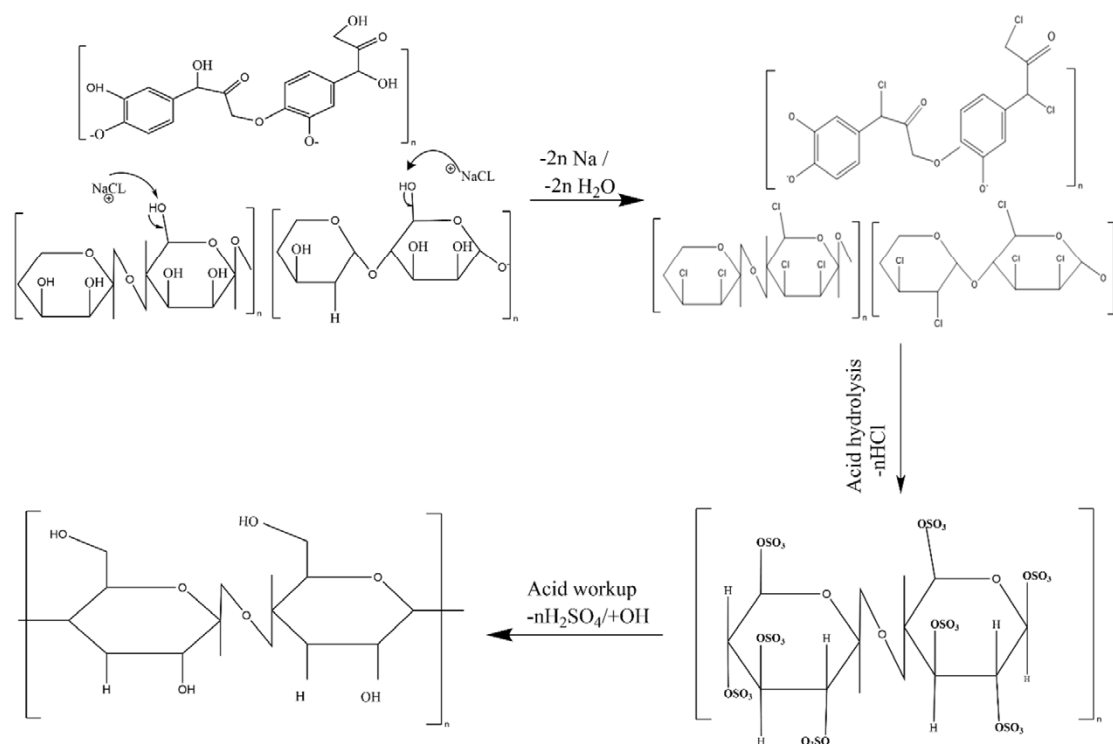
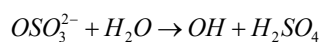
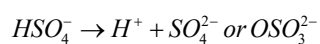
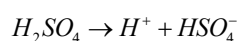


Fig. 3. Mechanism of Nanocellulose Extraction

depending on treatment time and concentration. When sodium hydroxide is treated with raw cotton straw, sodium hydroxide break down into sodium ions and hydroxide ion then they attach with lignin, cellulose, and hemicellulose and sodium ions are left into solution. Now, fiber had an effective surface to treat with sodium chlorite (Bleaching agent). The material was treated with sodium chlorite for the extraction of pure cellulose. Hydroxyl compounds are replaced with chlorite ions and form white smooth surface material. Again the material is neutralized with distilled water to overcome the bleaching process. At last, when the extracted material is treated with 40% H_2SO_4 then, the material starts to degrade and the Chlorite molecule was replaced with OSO_3^{2-} the material is turned into yellow color due to acid concentration. When we did acid workup then all OSO_3^{2-} were replaced with hydroxide ion and pure cellulosic material is formed. Acid hydrolysis follows the reaction given below:



Here, H_2SO_4 is acidic but when we treated it with cellulose material then it loses H^+ ion become basic by forming OSO_3^{2-} as a product. Now, OSO_3^{2-} is replaced with OH^- ion when we neutralize the solution with distilled water (shown in Fig. 3).

Characterization of Nanocellulose

The extracted material was characterized by FTIR (Fourier Transform Infrared Spectroscopy) for chemical composition, XRD (X-ray Diffraction) for the crystallinity of material, and FESEM (Field Emission Scanning Electron microscopy) for surface morphology analysis, TGA (Thermogravimetric analysis) to measure the thermal stability, DSC (Differential scanning calorimetry) to measure the energy absorbed and released by a sample. TEM (Transmission Electron Microscopy) for size and structural morphology.

Fourier Transform Infrared-Spectroscopy

Five spectra were examined for raw material (C1), alkali treatment (C2), bleaching treatment (C3), acid treatment (C4), and nanocellulose (C5)

Table 2. FTIR Reading of Cotton Straw Material

| Frequency | Functional group | Raw Material (C1) | Alkali Treatment (C2) | Bleaching (C3) | Acid Treatment (C4) | Nanocellulose (C5) | Reference |
|-----------|-----------------------------|-------------------|-----------------------|----------------|---------------------|--------------------|-----------|
| 4000-3000 | OH stretching | 3422.19 | 3419.43 | 3863.31 | 3385.50 | 3857.28 | [34] |
| | | 3857.28 | | 3742.71 | | 3421.42 | |
| 3000-2500 | C-H | 2928.64 | 2922.61 | 2928.64 | | 2901.82 | [2] |
| 2000-1650 | C=O | 1737.85 | 1728.81 | 1725.80 | 1725.80 | 1734.83 | [35] |
| 1670-1600 | C=C | 1632.92 | 1638.41 | 1641.43 | | 1650.47 | [36] |
| 1600-1300 | N-O | 1436.53 | 1433.52 | 1430.50 | | 1436.53 | [37] |
| | | | 1352.16 | | | 1319.02 | |
| 1400-1000 | O-H bonding | 1243.69 | 1231.63 | | 1288.88 | 1165.34 | [38] |
| | | 1108.09 | 1162.33 | 1165.34 | 1168.36 | 1114.12 | |
| | | 1053.37 | 1111.11 | 1053.78 | 1050.84 | 1057.88 | |
| | | | 1053.79 | | | | |
| 1000-650 | β -glycosidic linkage | 900.18 | 891.14 | 827.87 | 885.12 | 894.13 | [39] |
| | | 822.87 | 665.16 | 668.17 | 851.97 | 668.17 | |
| | | 657.76 | | | | | |

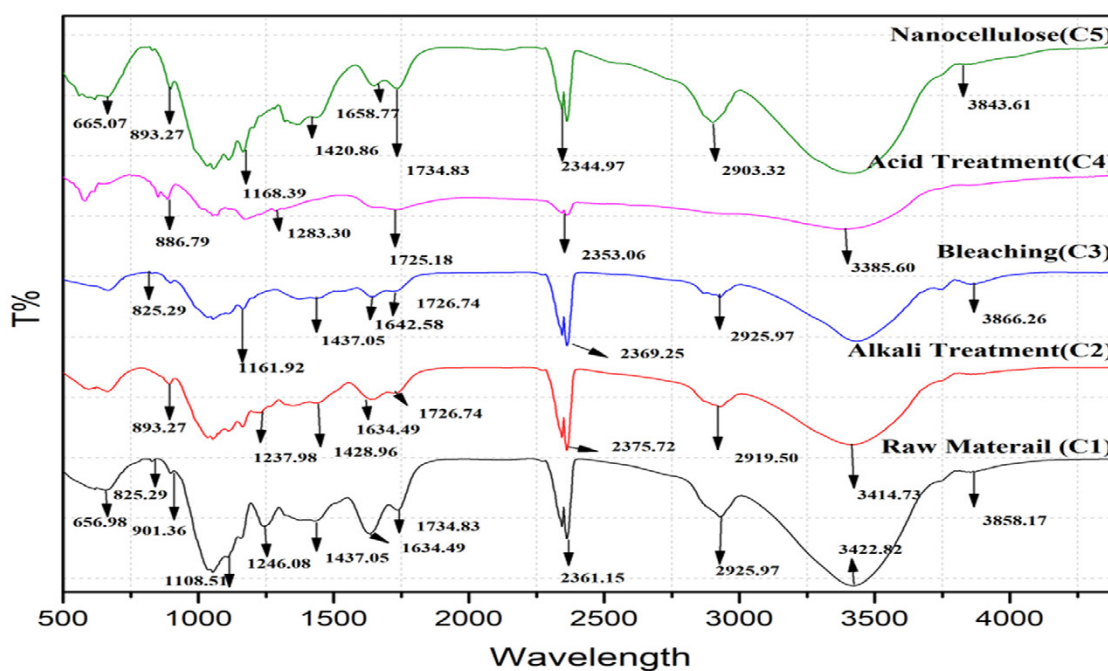


Fig. 4. FTIR analysis of processed samples

common peaks were obtained at different wavelengths as shown in Table 2. The wavelength of 1436.53cm^{-1} indicates the presence of cellulose (shown in Table 2 and Fig. 4) which shows approximately the value recorded in the extraction process of cotton straw nanocellulose analysis from 500 to 4400 cm^{-1} wavelength.

X-ray Diffraction

(XRD) is a fast methodical procedure used to generate a diffraction pattern whether the

material is crystalline or amorphous. The lower peak defines that the crystal is arranged in random order and the higher peak shows the desired crystal orientation. To characterize the crystallinity, the sample was scanned at 0° to 80° with 2θ angle. Cotton straw recorded the high-intensity diffraction peak approx. at diffraction angle $2\theta=22^\circ$ and scattered at amorphous part of sample approx. at $2\theta=18^\circ$. Similar results of diffraction peak $2\theta=20^\circ, 22^\circ, 15.1^\circ$ (110), 16.9° (110), and 23.0° (200) are recorded in nanocellulose which was

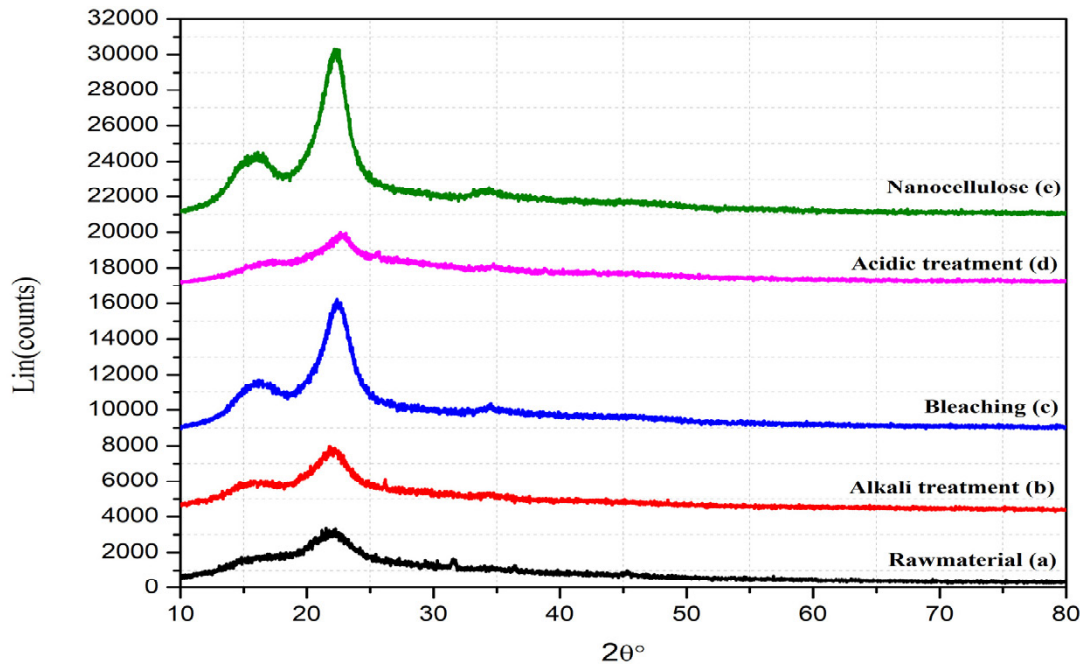


Fig. 5. The XRD pattern of a processed sample

Table 3. CrI value of cotton straw material

| Sample | CrI(%) |
|------------------|--------|
| Raw material | 43% |
| Alkali treatment | 26% |
| Bleaching fibers | 31% |
| Acid hydrolysis | 6% |
| Nanocellulose | 23% |

extracted from cotton cellulose with high-pressure homogenization[39-40]. In XRD data, raw material and alkali treatment material are amorphous which indicates the reflection or diffraction is not a particular place. Bleached fiber shows crystallinity at high-intensity peaks which resulted in the material being arranged in a specific order. Again Crystallinity is disappeared when we treated the material with 40 %(w/v) H₂SO₄.So, nanocellulose has a slight amorphous structure due to the arrangement of particles in random order and this was shown by low intensity and broad peaks while high-intensity peak shows the crystallinity of the material. CrI value was calculated with the equation such as:

$$CrI = \frac{I_{(002)} - I_{(AM)}}{I_{(002)}} \times 100$$

Whereas, I(Cr) measure for crystallinity of material and I(am) for the amorphous nature of the material. The results of CrI value and crystallinity structure are shown in (Table 3 and Fig. 5).

Field Emission Scanning Electron Microscopy

FESEM helps to analyze the shape, dimensional structure and recorded the surface morphology of cotton straw residue at 2 different stages Fig. 6(a) raw material and 6(b) nanocellulose extracted by acid hydrolysis with 40% (w/v) H₂SO₄ at 40°C for 1-hour FESEM records even and elongated fiber in the raw material of cotton waste. Fig 6(a) shows the raw material is recorded as a rough surface by using 10kV energy for FESEM analysis and Fig. 6(b) was recorded the surface is smooth and pores are present on the surface. In Tables 4(a) and 4(b) surface morphology was calculated by using Image J software of raw material in the standard form at

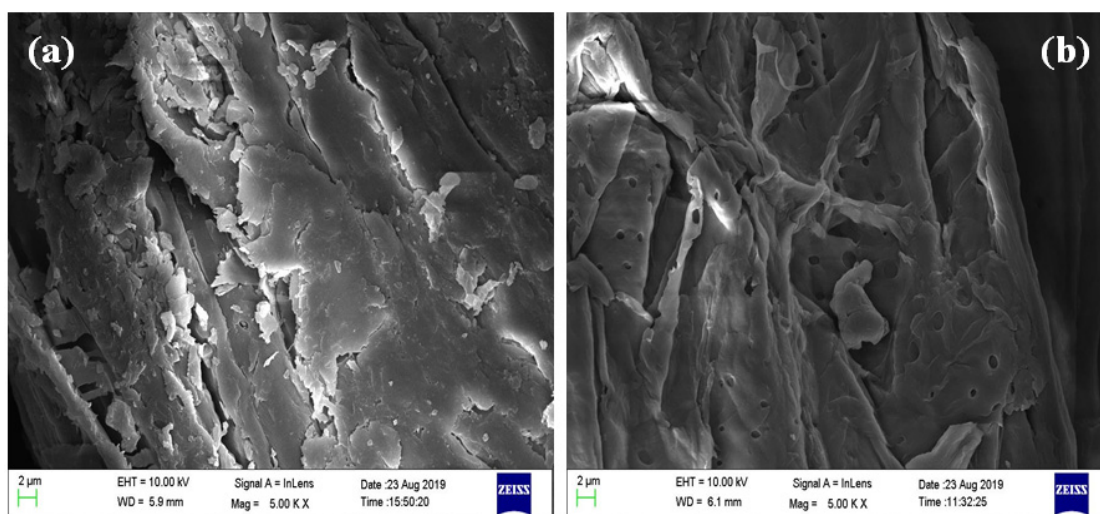


Fig. 6. (a) Raw material, (b) Nanocellulose

Table 4(a). FESEM image analysis of raw material

| Label | Area | Std.Dev. | Perimeter | Angle | Circularity | Integrated Density | Median | |
|-------|------------|------------|-----------|----------|-------------|--------------------|-------------|---------|
| 1 | 113846.154 | 41.834 | 2000 | -3.18 | 0.358 | 21677379.03 | 208.444 | |
| 2 | 187692.308 | 11.988 | 3330.05 | 29.982 | 0.213 | 13938051.22 | 70.5 | |
| 3 | 166153.846 | 17.591 | 2928.901 | -127.304 | 0.243 | 23221994.16 | 131.729 | |
| 4 | 193846.154 | 24.123 | 3417.601 | -103.134 | 0.209 | 22633087.3 | 109.364 | |
| 5 | 224615.385 | 42.618 | 3993.841 | 0 | 0.177 | 30929230.77 | 133 | |
| 6 | 193846.154 | 6.716 | 3446.291 | -3.691 | 0.205 | 11177866 | 55.871 | |
| 7 | 286153.846 | 11.294 | 5110.472 | 27.121 | 0.138 | 11776654.04 | 40.06 | |
| 8 | Mean | 195164.835 | 22.309 | 3461.022 | -25.744 | 0.22 | 19336323.22 | 106.996 |
| 9 | SD | 52694.112 | 14.664 | 952.328 | 63.063 | 0.069 | 7288043.893 | 57.751 |
| 10 | Min | 113846.154 | 6.716 | 2000 | -127.304 | 0.138 | 11177866 | 40.06 |
| 11 | Max | 286153.846 | 42.618 | 5110.472 | 29.982 | 0.358 | 30929230.77 | 208.444 |

Table 4(b). FESEM image analysis of nanocellulose

| Label | Area | Std.Dev. | Perimeter | Angle | Circularity | Integrated Density | Median | |
|-------|------------|------------|-----------|----------|-------------|--------------------|-------------|--------|
| 1 | 236923.077 | 110.474 | 2000 | -3.18 | 0.744 | 44892307.69 | 255 | |
| 2 | 483076.923 | 14.491 | 4320.969 | -119.197 | 0.325 | 33129230.77 | 69 | |
| 3 | 203076.923 | 26.17 | 1775.041 | 0 | 0.81 | 21553846.15 | 114 | |
| 4 | 335384.615 | 32.111 | 2892.962 | 122.471 | 0.504 | 28366153.85 | 101 | |
| 5 | 483076.923 | 22.474 | 4217.181 | -178.493 | 0.341 | 28707692.31 | 55 | |
| 6 | 415384.615 | 19.987 | 3672.769 | -25.017 | 0.387 | 37043076.92 | 90 | |
| 7 | 587692.308 | 20.652 | 5114.083 | -40.601 | 0.282 | 51430769.23 | 79 | |
| 8 | Mean | 392087.912 | 35.194 | 3427.572 | -34.86 | 0.485 | 35017582.42 | 109 |
| 9 | SD | 140462.545 | 33.643 | 1250.381 | 95.608 | 0.212 | 10327147.15 | 67.308 |
| 10 | Min | 203076.923 | 14.491 | 1775.041 | -178.493 | 0.282 | 21553846.15 | 55 |
| 11 | Max | 587692.308 | 110.474 | 5114.083 | 122.471 | 0.81 | 51430769.23 | 255 |

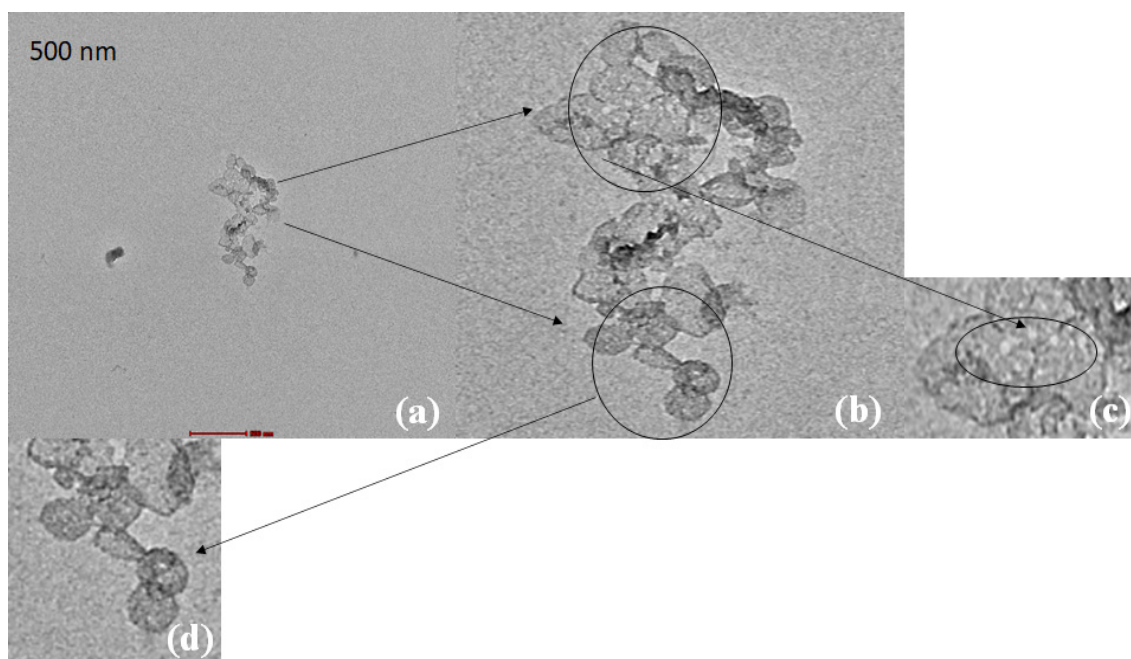


Fig. 7. Transmission Electron Microscopy analysis of the cotton straw nanocellulose.

magnification (5.00 kX) is 2000nm with electron high tension value at 20kV [42]. The mean area of raw material is 195164.835 and its mean integrated density is 19336323.22 (is the multiply of the area and mean gray value). If the Circularity value is 1 that indicates the material is perfectly circular, but here the value was recorded less than 1 which means the particle is in an irregular shape.

Transmission Electron Microscopy

To know the morphology, size, compositional structure, and texture of the material and the sample was magnified at 500 nm. TEM image of cotton straw nanocellulose pores was present on the surface as shown in Fig. 6(b). Crystals were arranged regularly.

TEM micrograph (a) exhibits polycrystalline material because of grain particles arrangement that shows irregular shape structure and small size particles. The particles are oriented in a different direction and arranged in random order. In the image (b) the particle is connected in a random order this is a magnified image to know the structure particle orientation. There are some pores at the surface which we already recognized before in the FESEM image and these pores are found all over the material so, both porous structure and

hollow structure are highly visible in the image (c). The structure of particles has irregular shapes with circular rod-like structures of different sizes.

Differential Scanning Calorimetry

It is used to measure the enthalpy variation or the behavior of the material as a function of temperature. The equipment measures the heat flow produced in a sample when it is heated, cooled, or held isothermally at a constant temperature. Nanocellulose was analyzed by using a platinum container and a 3g sample at 0-400°C with a heating rate of 10°C/min in Q-1, TA Instrument held in a helium atmosphere. Cotton straw nanocellulose showed a crystalline structure with enthalpy (411.33J/g) at 168.48°C and melting peak due to endothermic transition (shown in Fig. 8) and the similar result of Rosselle fiber has also been observed at 277.32-289.57°C [43].

Thermogravimetric Analysis

TGA used for the analysis of mean weight loss of the material is recorded as a function of weight and temperature, when the substance is heated at the final stage during the ignition then the weight of the substance is decreased with increasing the temperature. The thermal stability of nanocellulose is lower than lignocellulosic biomass such as

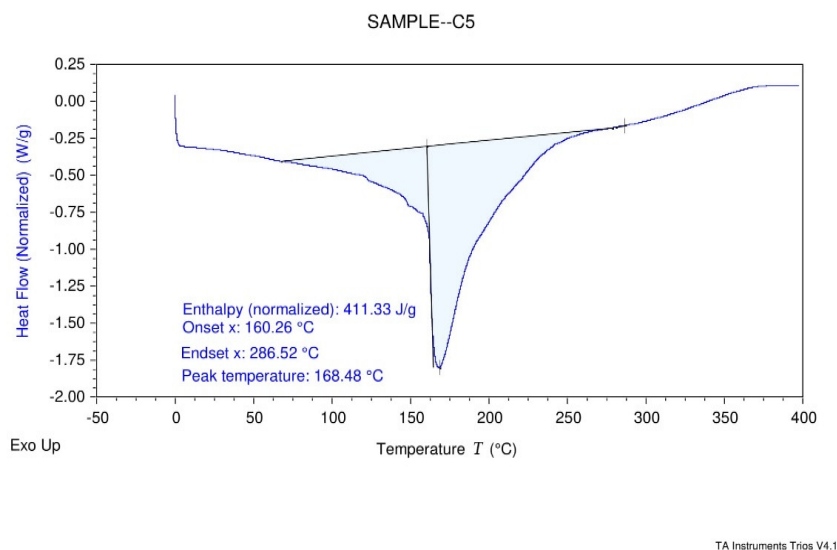


Fig. 8. Differential Scanning Calorimetry of nanocellulose

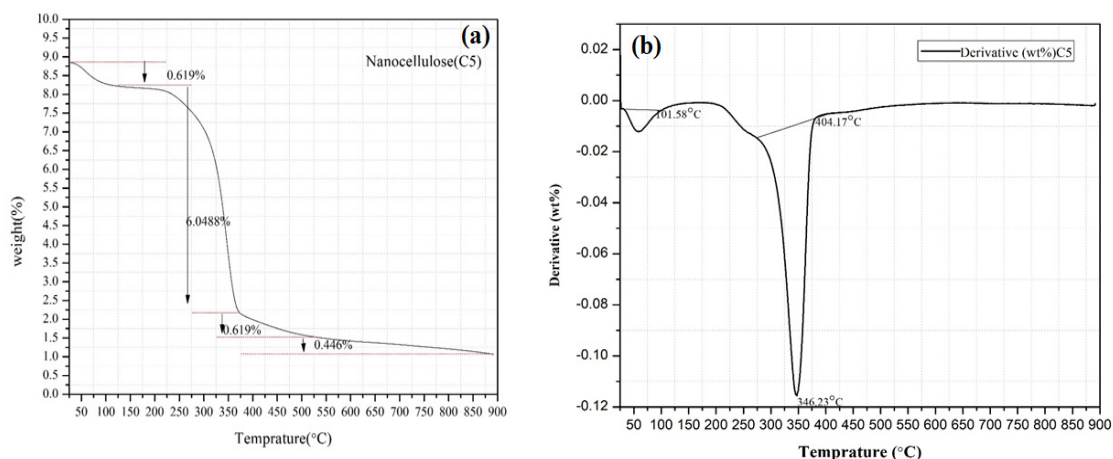


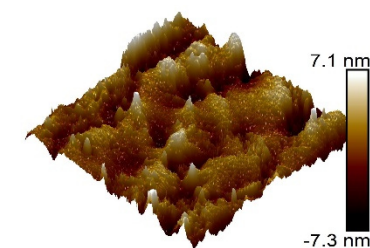
Fig.9. (a) Thermogravimetric analysis (b) Differential Thermogravimetric analysis

lignin, hemicellulose is eliminated after chemical treatment[36]. Four stages of thermal degradation were observed during the experiment (Fig. 9(a) and (b)). The weight loss (0.619%) was noticed at 25-150°C in the initial stage of the experiment. This may be due to the evaporation of moisture content. No degradation was observed between 150-190°C and a similar result has also been observed in lignocellulose biomass [44]. In the second stage during depolymerization, the weight loss (6.0488%) was noticed at the temperature range 200-375°C. At the third stage, samples were degraded from 375- 525°C with a weight loss of (0.619%). Finally, a rapid degradation with weight loss of (0.446%)

was noticed after 525°C. In Fig. 9(b) DTG curve was recorded the nanocellulose has major thermal stability at 346.23°C and similar results have also been observed in jackfruit peel [45].

Atomic Force Microscopy

The surface was characterized by atomic force microscopy (AFM) at ambient temperature. Silicon tip with a diameter of 10 nm was used to scan the surface in tapping mode. Cotton straw nanocellulose is uniformly distributed, due to the treatment of 40% acidic solution [46]. The resolution for AFM images was 256× 256 pixels. After imaging, the surface was flattened and analyzed



Height

Fig .10. AFM image of nanocellulose

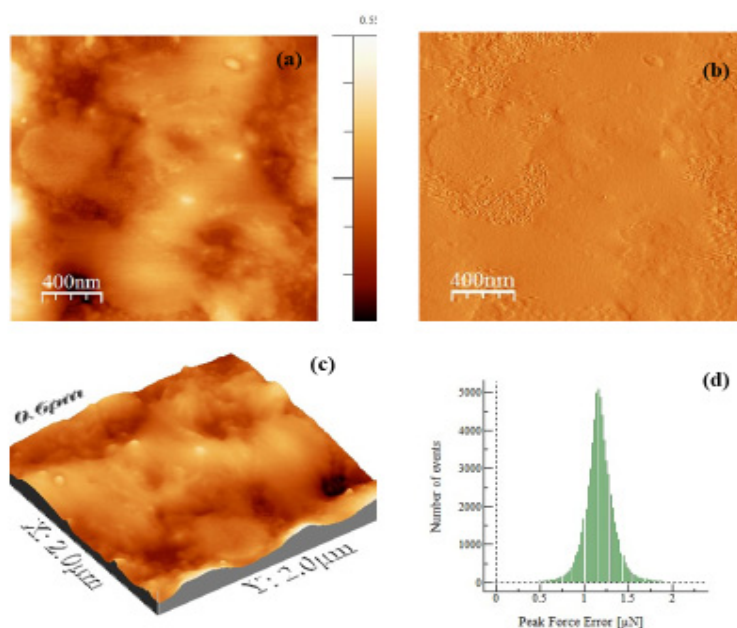


Fig .10. (a) Topographic image, (b) Phase image, (c) Three-dimensional structure,(d) Roughness surface variation

using WSxM software [47] to obtain the real height and phase image. The average height (1.2003 nm) of nanocellulose was calculated from the software. This indicates the ultra-smoothness of the surface. The root means square roughness(0.1738 nm) of the nanocellulose surface was calculated. This small value of roughness confirms the smoothness of the nanocellulose surface [48]. The size (7.1 nm)of nanocellulose was confirmed from AFM shown in Fig. 10. The detail of the topographic image, phase image, three-dimensional structure, and roughness surface variation is shown in Fig. 10(a-d).

CONCLUSION

The following conclusion has been made from the present study

1. Nanocellulose is extracted successfully with chemical method followed by ultrasonication and cryocrushing which helps the material to become nanosized with 23% crystallinity.
2. 1436.53cm^{-1} shows the presence of cellulose content extracted from cotton straw which has smooth surface morphology.
3. Particles of nanocellulose are irregular in shape with a circular rod-like structure.
4. Maximum weight loss of nanocellulose is found at $300\text{-}355^\circ\text{C}$.
5. Due to the removal of lignin, hemicellulose the thermal stability of crystalline material is decreased.
6. The size of nanocellulose was obtained at 7.1 nm.

CONFLICTS OF INTEREST

There are no conflicts to declare.

REFERENCE

- [1] B. M. Khadi and S. Venoor, "Cotton : An Introduction Chapter 1 Cotton : An Introduction," Springer, no. January 1970, 2015, doi: 10.1007/978-3-642-04796-1.
- [2] S. Shi, M. Zhang, C. Ling, W. Hou, and Z. Yan, "Extraction and characterization of microcrystalline cellulose from waste cotton fabrics via hydrothermal method," *Waste Manag.*, vol. 82, pp. 139–146, 2018, doi: 10.1016/j.wasman.2018.10.023.
- [3] S. N. Pandey and A. J. Shaikh, "Utilisation of cotton plant stalk for production of pulp and paper," *Biol. Wastes*, vol. 21, no. 1, pp. 63–70, 1987, doi: 10.1016/0269-7483(87)90147-9.
- [4] T. A. Gemtos and T. Tsiricoglou, "Harvesting of cotton residue for energy production," *Biomass and Bioenergy*, vol. 16, no. 1, pp. 51–59, 1999, doi: 10.1016/S0961-9534(98)00065-8.
- [5] J. Ma et al., "Fast adsorption of heavy metal ions by waste cotton fabrics based double network hydrogel and influencing factors insight," *J. Hazard. Mater.*, vol. 344, pp. 1034–1042, 2018, doi: 10.1016/j.jhazmat.2017.11.041.
- [6] H. Chen, X. Wang, J. Li, and X. Wang, "Cotton derived carbonaceous aerogels for the efficient removal of organic pollutants and heavy metal ions," *J. Mater. Chem. A*, vol. 3, no. 11, pp. 6073–6081, 2015, doi: 10.1039/c5ta00299k.
- [7] I. P. Sharma and C. Kanta, "Crop residues utilization : Wheat , paddy , cotton , sugarcane and groundnut," no. May, 2018.
- [8] A. Zoghalmi and G. Paës, "Lignocellulosic Biomass: Understanding Recalcitrance and Predicting Hydrolysis," *Front. Chem.*, vol. 7, no. December, 2019, doi: 10.3389/fchem.2019.00874.
- [9] A. García, A. Gandini, J. Labidi, N. Belgacem, and J. Bras, "Industrial and crop wastes: A new source for nanocellulose biorefinery," *Ind. Crops Prod.*, vol. 93, pp. 26–38, 2016, doi: 10.1016/j.indcrop.2016.06.004.
- [10] S. Achinas and G. J. W. Euverink, "Consolidated briefing of biochemical ethanol production from lignocellulosic biomass," *Electron. J. Biotechnol.*, vol. 23, pp. 44–53, 2016, doi: 10.1016/j.ejbt.2016.07.006.
- [11] P. Phanthong, P. Reubroycharoen, X. Hao, G. Xu, A. Abudula, and G. Guan, "Nanocellulose: Extraction and application," *Carbon Resour. Convers.*, vol. 1, no. 1, pp. 32–43, 2018, doi: 10.1016/j.crcon.2018.05.004.
- [12] M. Akram Khan, S. Guru, P. Padmakaran, D. Mishra, M. Mudgal, and S. Dhakad, "Characterisation studies and impact of chemical treatment on mechanical properties of sisal fiber," *Compos. Interfaces*, vol. 18, no. 6, pp. 527–541, 2011, doi: 10.1163/156855411X610250.
- [13] H. Kargazadeh, M. Ioelovich, I. Ahmad, S. Thomas, and A. Dufresne, "Methods for Extraction of Nanocellulose from Various Sources," *Handb. Nanocellulose Cellul. Nanocomposites*, pp. 1–49, 2017, doi: 10.1002/9783527689972.ch1.
- [14] J. Leitner, B. Hinterstoisser, M. Wastyn, J. Keckes, and W. Gindl, "Sugar beet cellulose nanofibril-reinforced composites," *Cellulose*, vol. 14, no. 5, pp. 419–425, 2007, doi: 10.1007/s10570-007-9131-2.
- [15] B. Soni, E. B. Hassan, and B. Mahmoud, "Chemical isolation and characterization of different cellulose nanofibers from cotton stalks," *Carbohydr. Polym.*, vol. 134, pp. 581–589, 2015, doi: 10.1016/j.carbpol.2015.08.031.
- [16] A. Chakraborty, M. Sain, and M. Kortschot, "Cellulose microfibrils: A novel method of preparation using high shear refining and cryocrushing," *Holzforchung*, vol. 59, no. 1, pp. 102–107, 2005, doi: 10.1515/HF.2005.016.
- [17] D. Bandera et al., "Influence of mechanical treatments on the properties of cellulose nanofibers isolated from microcrystalline cellulose," *React. Funct. Polym.*, vol. 85, pp. 134–141, 2014, doi: 10.1016/j.reactfunctpolym.2014.09.009.
- [18] K. Uetani and H. Yano, "Nanofibrillation of wood pulp using a high-speed blender," *Biomacromolecules*, vol. 12, no. 2, pp. 348–353, 2011, doi: 10.1021/bm101103p.
- [19] A. Ferrer, I. Filpponen, A. Rodríguez, J. Laine, and O. J. Rojas, "Valorization of residual Empty Palm Fruit Bunch Fibers (EPFBF) by microfluidization: Production of nanofibrillated cellulose and EPFBF nanopaper," *Bioresour. Technol.*, vol. 125, pp. 249–255, 2012, doi: 10.1016/j.biortech.2012.08.108.
- [20] S. Panthapulakkal and M. Sain, "Preparation and characterization of cellulose nanofibril films from wood fibre and their thermoplastic polycarbonate composites," *Int. J. Polym. Sci.*, vol. 2012, 2012, doi: 10.1155/2012/381342.
- [21] A. N. Frone, D. M. Panaitescu, D. D. Spataru, C. Radovici, R. Trusca, and R. Somoghi, "Preparation and characterization of PVA composites with cellulose nanofibers obtained by ultrasonication," *BioResources*, vol. 6, no. 1, pp. 487–512, 2011, doi: 10.15376/biores.6.1.487-512.
- [22] M. Martelli-Tosi, M. D. S. Torricillas, M. A. Martins, O. B. G. De Assis, and D. R. Tapia-Blácido, "Using Commercial Enzymes to Produce Cellulose Nanofibers from Soybean Straw," *J. Nanomater.*, vol. 2016, 2016, doi: 10.1155/2016/8106814.
- [23] N. Jain, A. Bhatia, and H. Pathak, "Emission of air pollutants from crop residue burning in India," *Aerosol Air Qual. Res.*, vol. 14, no. 1, pp. 422–430, 2014, doi: 10.4209/aaqr.2013.01.0031.
- [24] H. K. Goering and P. J. Van, "Forage fiber analyses," *U.S. Dep. Agric.*, no. 379, pp. 387–598, 1975.
- [25] P. J. Van Soest, J. B. Robertson, and B. A. Lewis, "Methods for Dietary Fiber, Neutral Detergent Fiber, and Nonstarch Polysaccharides in Relation to Animal Nutrition," *J. Dairy Sci.*, vol. 74, no. 10, pp. 3583–3597, 1991, doi: 10.3168/jds.S0022-0302(91)78551-2.
- [26] S. Nam, A. D. French, B. D. Condon, and M. Concha, "Segal crystallinity index revisited by the simulation of X-ray diffraction patterns of cotton cellulose I β and cellulose II," *Carbohydr. Polym.*, vol. 135, no. November, pp. 1–9, 2016, doi: 10.1016/j.carbpol.2015.08.035.
- [27] P. K. Keshav, N. Shaik, S. Koti, and V. R. Linga, "Bioconversion of alkali delignified cotton stalk using two-stage dilute acid hydrolysis and fermentation of detoxified hydrolysate into ethanol," *Ind. Crops Prod.*, vol. 91, no. April 2018, pp. 323–331, 2016, doi: 10.1016/j.indcrop.2016.07.031.
- [28] "Modified Van Soest method for lignocellulosic content analysis Reagents," no. I, pp. 4–5, 2017.
- [29] Z. Daud et al., "Analysis the Chemical Composition and Fiber Morphology Structure of Corn Stalk," vol. 7, no. 9, pp. 401–405, 2013.
- [30] P. Binod et al., "Bioethanol production from rice straw: An overview," *Bioresour. Technol.*, vol. 101, no. 13, pp. 4767–4774, 2010, doi: 10.1016/j.biortech.2009.10.079.
- [31] B. T. Shawky, M. G. Mahmoud, E. A. Ghazy, M. M. S. Asker,

- and G. S. Ibrahim, "Enzymatic hydrolysis of rice straw and corn stalks for monosugars production," *J. Genet. Eng. Biotechnol.*, vol. 9, no. 1, pp. 59–63, 2011, doi: 10.1016/j.jgeb.2011.05.001.
- [32] B. Yu et al., "Simultaneous isolation of cellulose and lignin from wheat straw and catalytic conversion to valuable chemical products," *Appl. Biol. Chem.*, vol. 64, no. 1, 2021, doi: 10.1186/s13765-020-00579-x.
- [33] M. Kiaei, A. Samariha, and J. E. Kasmani, "qvw," *African J. Agric. Res.*, vol. 6, no. 16, pp. 3762–3767, 2011, doi: 10.5897/AJAR10.752.
- [34] N. F. Mat Zain, "Preparation and Characterization of Cellulose and Nanocellulose From Pomelo (*Citrus grandis*) Albedo," *J. Nutr. Food Sci.*, vol. 05, no. 01, pp. 10–13, 2014, doi: 10.4172/2155-9600.1000334.
- [35] I. K. I. Al-khateeb, S. M. Hussin, and Y. M. Al-obaidi, "Extraction of Cellulose Nano Crystalline from Cotton by Ultrasonic and Its Morphological and Structural Characterization," *Int. J. Mater. Chem. Phys.*, vol. 1, no. 2, pp. 99–109, 2015.
- [36] L. Zhou, H. He, C. Jiang, L. Ma, and P. Yu, "Cellulose Nanocrystals from Cotton Stalk for Reinforcement of Poly(Vinyl Alcohol) Composites," *Cellul. Chem. Technol.*, vol. 51, no. 1, pp. 109–119, 2017, [Online]. Available: https://www.researchgate.net/publication/323414925_Cellulose_Nanocrystals_from_Cotton_Stalk_for_Reinforcement_of_PolyVinyl_Alcohol_Composites.
- [37] T. Theivasanthi, F. L. A. Christma, A. J. Toyin, S. C. B. Gopinath, and R. Ravichandran, "Synthesis and characterization of cotton fiber-based nanocellulose," arXiv, 2019.
- [38] M. Li, B. He, Y. Chen, and L. Zhao, "Physicochemical Properties of Nanocellulose Isolated from Cotton Stalk Waste," *ACS Omega*, vol. 6, no. 39, pp. 25162–25169, 2021, doi: 10.1021/acsomega.1c02568.
- [39] Kusmono, R. F. Listyanda, M. W. Wildan, and M. N. Ilman, "Preparation and characterization of cellulose nanocrystal extracted from ramie fibers by sulfuric acid hydrolysis," *Heliyon*, vol. 6, no. 11, p. e05486, 2020, doi: 10.1016/j.heliyon.2020.e05486.
- [40] Y. Wang, X. Wei, J. Li, Q. Wang, F. Wang, and L. Kong, "Homogeneous Isolation of Nanocellulose from Cotton Cellulose by High Pressure Homogenization," *J. Mater. Sci. Chem. Eng.*, vol. 01, no. 05, pp. 49–52, 2013, doi: 10.4236/msce.2013.15010.
- [41] M. Mariño, L. L. Da Silva, N. Durán, and L. Tasic, "Enhanced materials from nature: Nanocellulose from citrus waste," *Molecules*, vol. 20, no. 4, pp. 5908–5923, 2015, doi: 10.3390/molecules20045908.
- [42] R. K. Gond, M. K. Gupta, and M. Jawaid, "Extraction of nanocellulose from sugarcane bagasse and its characterization for potential applications," *Polym. Compos.*, vol. 42, no. 10, pp. 5400–5412, 2021, doi: 10.1002/pc.26232.
- [43] L. K. Kian and M. Jawaid, "Thermal properties of nanocrystalline cellulose and cellulose nanowhisker," *Int. J. Innov. Technol. Explor. Eng.*, vol. 9, no. 1, pp. 5430–5434, 2019, doi: 10.35940/ijitee.A8103.119119.
- [44] H. Yang, R. Yan, H. Chen, D. H. Lee, and C. Zheng, "Characteristics of hemicellulose, cellulose and lignin pyrolysis," *Fuel*, vol. 86, no. 12–13, pp. 1781–1788, 2007, doi: 10.1016/j.fuel.2006.12.013.
- [45] C. Trilokesh and K. B. Uppuluri, "Isolation and characterization of cellulose nanocrystals from jackfruit peel," *Sci. Rep.*, vol. 9, no. 1, pp. 1–8, 2019, doi: 10.1038/s41598-019-53412-x.
- [46] Z. Liu, M. He, G. Ma, G. Yang, and J. Chen, "Preparation and characterization of cellulose nanocrystals from wheat straw and corn stalk," *Palpu Chongi Gisul/Journal Korea Tech. Assoc. Pulp Pap. Ind.*, vol. 51, no. 2, pp. 40–48, 2019, doi: 10.7584/JKTAPPI.2019.04.51.2.40.
- [47] I. Horcas, R. Fernández, J. M. Gómez-Rodríguez, J. Colchero, J. Gómez-Herrero, and A. M. Baro, "WSXM: A software for scanning probe microscopy and a tool for nanotechnology," *Rev. Sci. Instrum.*, vol. 78, no. 1, 2007, doi: 10.1063/1.2432410.
- [48] B. K. Parida and S. Sarkar, "Stoichiometric influences on ion beam nanopatterning of CoSi binary compound," *Vacuum*, vol. 175, no. September 2019, p. 109246, 2020, doi: 10.1016/j.vacuum.2020.109246.